Thermodynamic analysis of a combined ORC-TFC cycle for power generation from low-temperature energy sources by using Excel

Abstract

This paper presents a thermodynamic evaluation of a combined power generation cycle for utilising the energy of low-temperature heat sources such as solar energy and industrial waste energy. The cycle connects the simple Organic Rankine Cycle (ORC) with the Trilateral Flash Cycle (TFC) via a cascade condenser. By applying the TFC in the high-temperature circuit and the ORC in the low-temperature circuit, the combined cycle enjoys the merits of the two subsidiary cycles. For evaluating the thermodynamic performance of the cycle, an Excel-based model is used that determines the fluid properties by using special functions developed with Microsoft's Visual Basic for Applications (VBA). The performance of the combined cycle is compared with those of the simple TFC and ORC for a heat-source available at 120^{o}C and various values of the cascade-condenser temperature by using R152a as the refrigerant in all three cycles.

Keywords: Organic Rankine cycle, trilateral flash cycle, low-temperature energy sources, Microsoft Excel, VBA

1. Introduction

The mounting concerns about the damage to the environment and the climate changes due to the use of fossil-fuels for electricity generation have inspired intensive research for the development of new technologies that utilise alternative energy sources such as solar and geothermal energy and waste heat from industries. One of the promising technologies for the utilisation of such energy sources is the organic Rankine cycle (ORC) [1,2]. Unlike the conventional Rankine cycle that requires steam at very high temperatures before expanding in the turbine, the ORC can be adapted to heat sources at low and moderate temperatures by using an organic working fluid instead of steam. Efficiency is the main concern about the cycle and, like the conventional cycle, various modifications to the simple ORC have been considered for improving it such as reheating, regeneration, and recuperation [3]. Although such modifications proved to be effective, they do not address an inherent drawback of the ORC which is the mismatch between the temperature of a finite heating source and that of the working fluid during the heat-addition process in the evaporator since the temperature of the working fluid remains constant while that of the heating source drops [4]. To solve this problem, the trilateral flash cycle has been proposed. In this cycle, the heat recovery process is not allowed to vaporise the working which is taken directly as saturated liquid to expand in a two-phase expander [4-7]. The problem with the TFC is that the technology of expanders is relatively immature and, therefore, they are less efficient compared to the conventional turbines [3]. According to [4, 5, and 6], the two-phase expander is the main factor for degrading the efficiency of the TFC.

Many previous researchers developed theoretical models for evaluating the performance of the ORC and TFC from thermodynamics and thermoeconomic viewpoints. For example, Bidgoli and Yanagihara [2] analysed an ORC system to recover the waste heat from the intercoolers of the compression units of a large processing plant. By using Aspen HYSYS, they compared the performance of various working fluids including R123, n-butane, n-pentane, hexane, and n-heptane. Their results showed that a net power of up to 40 MW could be generated with R123. Wolf et al. [1] investigated a solar powered ORC using pure iso-pentane and two iso-pentane/CO_2 zeotropic mixtures. Modelling of the system was done by using the Engineering Equation Solver (EES) software and determining the thermodynamic properties by using REFPROP. Their exergy and exergo-economic analyses showed that the investigated unit was capable of co-producing approximately 30 kW electricity and 160 kW district heating with a exergetic efficiency exceeding 60%. Therefore, they concluded that the unit was able to compete with existing renewable power generating systems in terms of specific cost of electricity.

Yari et al. [5] considered a low-grade heat source with a temperature of 120°C and conducted parametric studies for several working fluids in ORC and TFC cycles by using the EES software. Their results showed that increasing the inlet temperature of the TFC expander increases the net output power and decreases the product cost, but this was not the case for the ORC system. Lykas et al. [6] compared two organic cycles feeding with the same low-temperature (80-100°C) heat source. The first cycle was an ORC in which a small fraction of the supplied waste heat was continuously provided to the expander with the aim of approaching a quasi-isothermal process instead of the adiabatic one. The second cycle was the TFC. They performed parametric thermodynamic analyses of the two cycles, with R1234ze(E), R1234yf, R1233zd(E), and R134a as working fluids by using Aspen Plus software. Their techno-economic study of the first cycle conducted by using Aspen Process Economic Analyzer (APEA) with the four working fluids showed that R1233zd(E) was the most proper working fluid for the cycle.

The combination of the ORC with another cycle was also studied by some researchers. For example, Sun et al. [8] investigated the ORC cycle combined with the Absorption Refrigeration Cycle (ARC) and the Ejector Refrigeration Cycle (ERC) to recover the waste heat from the flue gas for generating both power and cooling for external uses. Their results, with R113 as the working fluid, showed that the net power output, refrigerating capacity, and exergy efficiency of the ORC-ARC combination are all higher than those of the ORC-ERC combination for evaporation temperatures of the basic ORC exceeding 153°C. Toujani et al. [9] combined the ORC with the vapour compression refrigeration (VCR) cycle for cogeneration with a negative cold (-10–0°C) and a positive cold (0–10°C) applications. By using n-hexane as working fluids for the ORC and R600 for the VCC, they examined three configurations in terms of the net power, refrigeration capacity and overall efficiency. Their results obtained by using the EES software showed that, for a hot spring of 1000 kW, the cycle could provide simultaneously, a maximum net work of 17 kW and a maximum net cooling capacity of 160 kW at an overall coefficient of the order of 0.3. For the production of positive cold, their results showed that the basic ORC cycle (without recovery) was the most suitable option.

Other researchers reported the results of theoretical studies of cascade ORC systems or hybrid systems involving ORC with steam turbines. For example, Oko et al. [10] presented exergoeconomic analysis of a 100 kW solar driven ORC power plant. They considered a cascade cycle of R134a and R290 as working fluids and developed their model in Microsoft Excel and MATLAB environments. They determined the energy and exergy efficiencies of the proposed plant at the optimal collector operation as 18.92 and 21.61%, respectively. Liu et al. [11] used EES software to study a two stage subcritical saturated ORC system with a heat source temperature of 100~150^{o}C with four different organic working fluids. Najjar and Qatramez [12] modelled a hybrid system consisting of a single flash geothermal cycle operating on a steam turbine and ORC using n-butane, isobutane, R11, and R123. The highest energy efficiency of 18.76% and net power output of 24,887MW were obtained with R11. Mokarram and Mosaffa [13] studied a cycle that integrated a steam turbine and a trans-critical ORC using R245fa. They showed that the system could produce 7.2% more power compared to a similar cycle operating in subcritical conditions. With a maximum energy and exergy efficiencies of 14.66% and 55.15%, respectively, the system's levelised cost of energy (LCOE) was 0.2018 USD/kWh.

The brief literature review given above and the more comprehensive review given in [14] indicate that a cycle that combines the TFC in the high-temperature circuit (HTC) and the ORC in the low-temperature circuit (LTC) has not been considered before. While minimising the mismatch between the working fluid and the heat source for the ORC, this cycle enables a turbine to be used in the LTC instead of the two-phase expander. Moreover, different organic fluids can be used in the HTC and LTC that suit the high and low temperature ranges better than a single fluid. Needless to say that such a cycle also gives cogeneration systems more flexibility than a single ORC or LTC. In this regard, the present paper contributes to knowledge by presenting a thermodynamic evaluation of this new cycle. From another perspective, the literature review shows that most researchers used commercial software for their analyses. However, the use of general-purpose software can encourage independent researchers and engineering students to contribute to the development of innovative ORC and TFC systems using suitable fluids [15, 16]. In this respect, the present study uses Microsoft Excel as the modelling platform with special VBA functions to determine the thermodynamic properties of the working fluids. While the versatile solver that comes with Excel can be used for single-objective optimisation analyses, the free version of the MIDACO solver [17] or the Solver-TOPSIS technique described in [18] can be used for multi-objective optimisation analyses

2. The ORC, TFC, and the proposed combined ORC-TFC cycle

Figure 1 shows schematic diagrams of the simple ORC and TFC systems and Figure 2 shows their respective T-s diagrams. As Figure 1.a shows, the ORC system has the same components as those of the conventional Rankine cycle which are the evaporator (boiler), the turbine, the condenser, and the pump. Organic fluids are used in the ORC instead of water because they have higher boiling pressures at low temperatures and, therefore, suit the low-temperature applications better. To avoid the problem of blade erosion at the last turbine stages, dry or isentropic fluids are usually selected for which the saturated liquid-vapour curves have negative or infinite slopes, respectively [3,13].

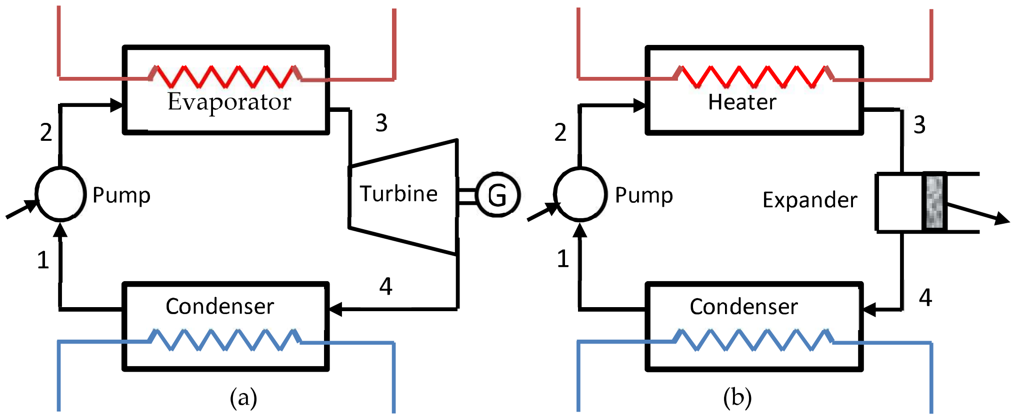

Figure 1: Schematic diagrams of: (a) the ORC system and (b) the TFC system

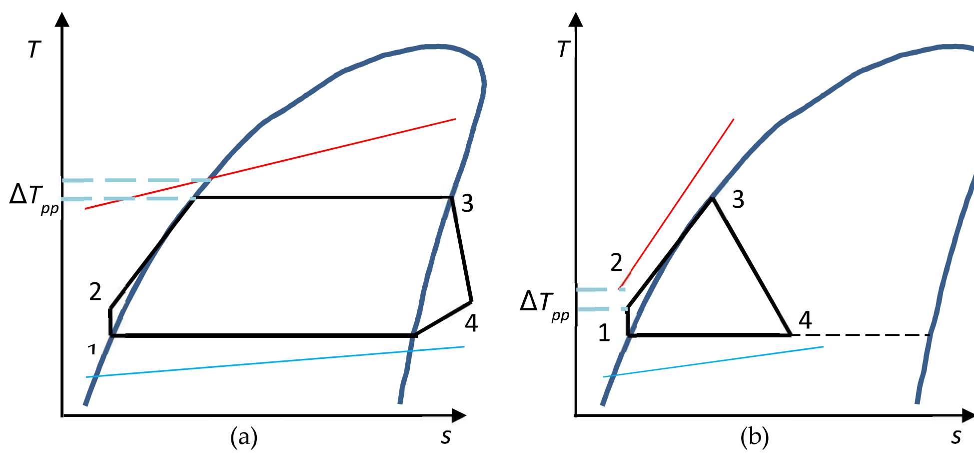

Figure 2: *T*-*s* diagrams of: (a) the ORC cycle and (b) the TFC cycle

The TFC system is different from the ORC system in that it heats the working fluid without going into the vaporisation process so that the hot pressurised fluid expands in the two-phase region. As Figure 2.b shows, this cycle leads to a uniform temperature glide between the heat source and the working fluid; which reduces the losses during the heat-transfer process and improves the performance of the TFC systems. Typically, TFC systems can provide 50% more work than ORC systems for the same energy input, but they need sophisticated expanders that can adequately handle the liquid-phase presence during the expansion process [3]. Apart from increasing the investment cost, two-phase expanders are generally less efficient than conventional vapour turbines.

Figure 3.a shows a schematic diagram of the combined-cycle system in which the heat source is first used to heat the working fluid of the TFC circuit and then heat the working fluid of the ORC circuit. After expanding in the two-phase expander to produce power, the working fluid of the TFC circuit is condensed by the cooler working fluid of the ORC circuit in a cascade condenser (cc) before being pumped into the TFC heater. The ORC system shown on Figure 3.a is a recuperative system in which

the superheated fluid exiting the turbine is used to heat the cold fluid exiting the pump in an internal heat-exchanger (IHEX). In the condenser, the working fluid is cooled by the cold-sink fluid to the saturated-liquid state and then pumped into the cold side of the IHEX. After the IHEX, the fluid is heated by the heat source to the state of saturated liquid before entering the cascade condenser where it is heated further by the condensing fluid of the TFC circuit until it becomes saturated vapour.

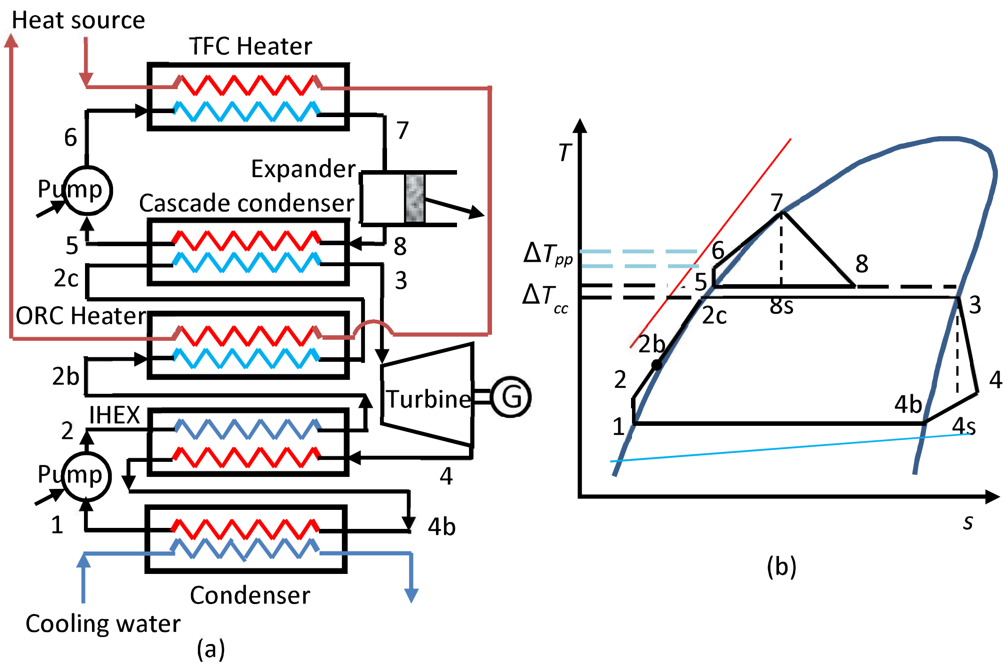

Figure 3: Schematic and *T-s* diagrams for the combined ORC-TFC cycle

Figure 3.b shows the *T-s* diagram of the combined cycle. Unlike the TFC cycle in which the pinch point occurs where the heating fluid exits the system, that of the combined cycle occurs in the middle of the heating process which forces the heating source to exit the system at a higher temperature than that of the TFC. Although this limits the amount of heat recovered and the work produced by the ORC circuit, the combined cycle can still produce more work than the simple ORC alone because of the additional work produced by the TFC circuit. Compared to a simple TFC, the combined cycle may not be able to produce the same power but it can have a higher thermal efficiency by replacing the two-phase expander with the single-phase turbine and by allowing two different working fluids to be used in the TFC and ORC circuits that lead to a better overall performance than a single fluid.

3. The analytical models

The analytical models applied for the present thermodynamic analyses assume steady-state operation and neglect pressure losses and heat-transfer losses in the various components. However, the losses due to irreversibility in the pumps, the turbine, and the two-phase expander are taken into consideration via the relevant isentropic efficiencies [19].

3.1. The analytical model for the TFC circuit

Given the pinch-point temperature difference, ΔT_{pp}, the temperature of the heat source exiting the heater of the TFC, $T_{hso,TFC}$, is determined from:

$$T_{hso,TFC} = T_6 + \Delta T_{pp} \tag{1}$$

Given the inlet temperature of the heat source, $T_{hs,in}$, and its mass flow rate, $\dot{m}_{hs}$, the rate of heat transfer from the heat source (a stream of hot-water) to the working fluid of the TFC, $\dot{Q}_{hs,TFC}$, and the mass flow rate of the working fluid, $\dot{m}_{TFC}$, are calculated from:

$$\dot{Q}_{hs,TFC} = \dot{m}_{hs} c_p \left(T_{hs,in} - T_{hso,TFC}\right) \tag{2}$$

$$\dot{m}_{TFC} = \dot{Q}_{hs,TFC} / \left(h_7 - h_6\right) \tag{3}$$

The specific work, in kJ per kg, of the working fluid in the TFC during the two-phase expansion process is evaluated from the enthalpy change as follows:

$$w_{exp} = \left(h_7 - h_{8s}\right) \times \eta_{exp} \tag{4}$$

Where, η_{exp} is the isentropic efficiency of the expander and h_{8s} is the enthalpy of the fluid after an isentropic expansion (refer to Figure 3.b). The TFC pump specific work is given by:

$$w_{p,TFC} = v_5 \left(p_{eva,TFC} - p_{cc,TFC}\right) / \eta_{p,TFC} \tag{5}$$

Where, $p_{eva,TFC}$ and $p_{cc,TFC}$ are the pressures of the TFC fluid in the evaporator and cascade-condenser, respectively. Equation (6) is then used to determine the enthalpy of the fluid at state 6 after the pump:

$$h_6 = h_5 + w_{p,TFC} \tag{6}$$

The thermal efficiency of the TFC circuit alone is given by:

$$\eta_{TFC} = \dot{m}_{TFC} \left(w_{exp} - w_{p,TFC}\right) / \dot{Q}_{hs,TFC} \tag{7}$$

3.2. The analytical model for the ORC circuit

Referring to Figure 3b, the mass flow rate of the working fluid in the ORC circuit is given by:

$$\dot{m}_{ORC} = \dot{m}_{TFC} \left(h_8 - h_5\right) / \left(h_3 - h_{2c}\right) \tag{8}$$

The pump specific work is given by:

$$w_{p,ORC} = v_1 \left(p_{cc,ORC} - p_{con,ORC}\right) / \eta_{p,ORC} \tag{9}$$

Where, $\eta_{p,ORC}$ is the isentropic efficiency of the ORC pump. Energy balance over the IHEX gives:

$$h_{2b} = h_2 + \left(h_4 - h_{4b}\right) \tag{10}$$

Where, h_{4b} is the enthalpy of the saturated vapour at the condenser pressure. The enthalpy h_4 is determined by taking into consideration the irreversibility of the turbine as follows:

$$h_4 = h_3 + (h_3 - h_{4s}) \times \eta_t \tag{11}$$

Where h_{4s} is the enthalpy after an isentropic expansion and η_t is the isentropic efficiency of the turbine. The turbine's specific work is then calculated from:

$$w_t = h_3 - h_4 \tag{12}$$

The thermal efficiency of the ORC circuit alone is given by:

$$\eta_{ORC} = \dot{m}_{ORC}(w_t - w_{p,ORC}) / \dot{Q}_{hs,TFC} \tag{13}$$

Where, $\dot{Q}_{hs,ORC}$ is the heat recovered in the ORC circuit, which is given by:

$$\dot{Q}_{hs,ORC} = \dot{m}_{ORC}(h_{2c} - h_{2b}) \tag{14}$$

3.3. The analytical model for the combined cycle

The total heat recovered from the heat source and total net power produced by the combined cycle, respectively, are given by:

$$\dot{Q}_{hs,tot} = \dot{Q}_{hs,TFC} + \dot{Q}_{hs,ORC} \tag{15}$$

$$\dot{W}_{tot} = \dot{m}_{ORC}(w_t - w_{p,ORC}) + \dot{m}_{TFC}(w_{exp} - w_{p,TFC}) \tag{16}$$

The overall thermal efficiency and the second-law (exergetic) efficiency of the cycle are given by:

$$\eta_{tot} = \dot{W}_{tot} / \dot{Q}_{hs,tot} \tag{17}$$

$$\varepsilon_{tot} = \dot{W}_{tot} / \dot{E}_{hs,in} \tag{18}$$

Where, $\dot{E}_{hs,in}$ in Equation (18) is the rate of exergy flow of the heat source entering the system following the definition adopted by Yari et al. [5]:

$$\dot{E}_{hs,in} = \dot{m}_{hs}\left[(h_{hs,in} - h_0) - T_0(s_{hs,in} - s_0)\right] \tag{19}$$

The temperature of the heat source exiting the system is given by:

$$T_{hs,out} = T_{hs,in} - \dot{Q}_{hs,tot} / \dot{m}_{hs} c_p \tag{20}$$

Where c_p is the specific heat of the heating medium.

4. Development of the Excel models

Excel-based models for the three cycles have been developed that determine the thermal fluid properties by using special user-defined functions developed with VBA [20]. The functions for saturated liquids and saturated vapours interpolate the data given by ASHRAE [21], but he functions that determine the enthalpy and entropy of superheated refrigerants use ideal-gas equations in which the specific heat is determined at an adjusted pressure by multiplying the actual pressure by a "compressibility factor" for which an average value of 0.5 is adopted [22]. The accuracy of this approximation that enables the functions to be used for supercritical conditions was verified by El-Awad et al. [22]. They assessed the functions' accuracy for the analyses of a simple VCR system by comparing their results with those obtained by Atalay and Conan [23] with REFPROP for two ozone-friendly refrigerants, R410A and R1234yf, and two natural refrigerants, R290 and, R744. El-Awad et al. [22] also analysed a cascade VCR system with R507A in the high-temperature circuit and R23 in the low-temperature circuit and compared the results of the functions with those obtained by Parekh and Tailor [24] who used EES.

4.1. The ORC model

Yari et al. [5] analysed the simple ORC with a heat source at 120oC with the data shown on Table 1 by using seven working fluids, which are: R134a, R1234yf and R152a, propane (R290), n-butane (R600), iso-butane (R600a), and ammonia (R717).

Table 1. Values of the parameters used for the simple ORC model [5]

Parameter	Value
T_{hs} (°C)	120
$\dot{m}_{hs}$ (kg/s)	100
T_{cond} (°C)	40
ΔT_{pp} (K)	10
η_p (%)	85
η_t (%)	85

Figure 4 shows the Excel-aided model developed for the simple ORC by using their data with R152a as the working fluid. The results of Yari et al. [5] showed that the ORC has a certain temperature in its evaporator that maximises its output power, which is 80°C. Therefore, this temperature is used in the present model as shown on Figure 4. The sheet consists of four blocks of cells.

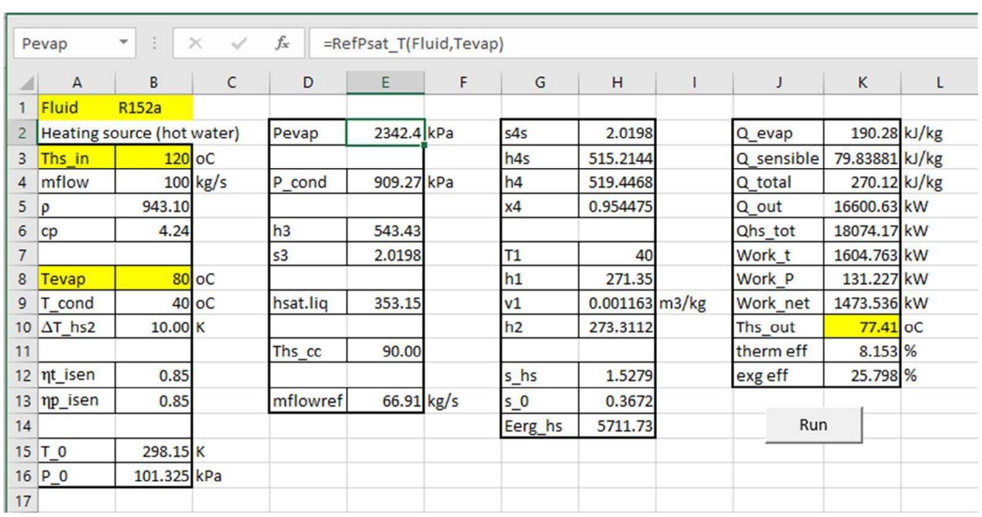
Pevap | =RefPsat_T(Fluid,Tevap)

	A	B	C	D	E	F	G	H	I	J	K	L
1	Fluid	R152a										
2	Heating source (hot water)			Pevap	2342.4	kPa	s4s	2.0198		Q_evap	190.28	kJ/kg
3	Ths_in	120	oC				h4s	515.2144		Q_sensible	79.83881	kJ/kg
4	mflow	100	kg/s	P_cond	909.27	kPa	h4	519.4468		Q_total	270.12	kJ/kg
5	ρ	943.10					x4	0.954475		Q_out	16600.63	kW
6	cp	4.24		h3	543.43					Qhs_tot	18074.17	kW
7				s3	2.0198		T1	40		Work_t	1604.763	kW
8	Tevap	80	oC				h1	271.35		Work_P	131.227	kW
9	T_cond	40	oC	hsat.liq	353.15		v1	0.001163	m3/kg	Work_net	1473.536	kW
10	ΔT_hs2	10.00	K				h2	273.3112		Ths_out	77.41	oC
11				Ths_cc	90.00					therm eff	8.153	%
12	ηt_isen	0.85					s_hs	1.5279		exg eff	25.798	%
13	ηp_isen	0.85		mflowref	66.91	kg/s	s_0	0.3672				
14							Eerg_hs	5711.73		Run		
15	T_0	298.15	K									
16	P_0	101.325	kPa									
17												

Figure 4: The Excel-aided model for the simple ORC with the data given by [5]

The first block on the left side of the sheet stores the specified data, while the second and third blocks in the middle perform the calculations for the ORC cycle. The fourth block on the right side of the sheet determines the overall cycle parameters that include the total amount of recovered heat (Qhs_tot), the net power produced by the system (Work_net), the exit temperature of the heating source (Ths_out), and the overall energetic (therm_eff) and exergetic (exg_eff) efficiencies. The name of the fluid is stored as a variable so that the model can also be used for fluids other than R152a.

4.2. The TFC model

Figure 5 shows the model developed for the TFC also using the input data of Table 1 and with R152a as the working fluid. The temperature of the fluid entering the TFC expander is taken as 110oC and the isentropic efficiency of the TFC expander is specified as 75%. The condenser temperature is 40oC and the pinch-point temperature difference is 10°C.

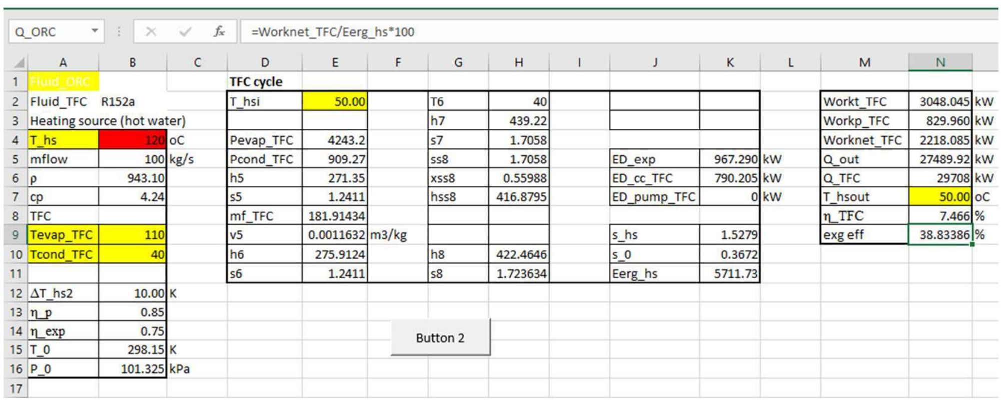

Q_ORC   =Worknet_TFC/Eerg_hs*100

	A	B	C	D	E	F	G	H	I	J	K	L	M	N	
1	Fluid_ORC			TFC cycle											
2	Fluid_TFC	R152a		T_hsi	50.00		T6	40					Workt_TFC	3048.045	kW
3	Heating source (hot water)						h7	439.22					Workp_TFC	829.960	kW
4	T_hs	120	oC	Pevap_TFC	4243.2		s7	1.7058					Worknet_TFC	2218.085	kW
5	mflow	100	kg/s	Pcond_TFC	909.27		ss8	1.7058		ED_exp	967.290	kW	Q_out	27489.92	kW
6	ρ	943.10		h5	271.35		xss8	0.55988		ED_cc_TFC	790.205	kW	Q_TFC	29708	kW
7	cp	4.24		s5	1.2411		hss8	416.8795		ED_pump_TFC	0	kW	T_hsout	50.00	oC
8	TFC			mf_TFC	181.91434								η_TFC	7.466	%
9	Tevap_TFC	110		v5	0.0011632	m3/kg				s_hs	1.5279		exg eff	38.83386	%
10	Tcond_TFC	40		h6	275.9124		h8	422.4646		s_0	0.3672				
11				s6	1.2411		s8	1.723634		Eerg_hs	5711.73				
12	ΔT_hs2	10.00	K												
13	η_p	0.85													
14	η_exp	0.75					Button 2								
15	T_0	298.15	K												
16	P_0	101.325	kPa												
17															

Figure 5: The Excel-aided model for the TFC using R152a with the data of Table 1

4.3. The combined-cycle model

Figure 6 shows the model developed for the combined cycle. The figure shows four blocks of cells the first of which on the left side of the sheet stores the specified data, while the second and third blocks in the middle perform the calculations for the TFC and ORC circuits, respectively. The fourth block on the right side of the sheet determines the overall cycle parameters. The figure shows that R152a is used in both the TFC and ORC circuits, but the names of the working fluids in the two circuits are treated as variables so that the model can be used for different fluid pairs. The temperature of the TFC fluid in the cascade condenser, Tcc_TFC, is specified as 83°C and the cascade-condenser temperature difference as 3°C. Therefore, the cascade-condenser temperature of the ORC fluid, Tcc_ORC, is 80°C.

By fixing value of the temperature of the TFC fluid entering the expander at 110°C, the power, thermal efficiency, and exergetic efficiency of the combined cycle were calculated at various values of the cascade-condenser temperature in the cycle with R152a as the single working fluid. The results are plotted on Figure 7 which shows that the thermal efficiency of the combined cycle increases steadily with the temperature of the ORC fluid in the cascade condenser, while its power drops. The figure also shows that the exergetic efficiency has a maximum value at the cascade temperature of 75oC. Clearly, the combined cycle has a certain cascade temperature that gives the best trade-off between its produced power, thermal efficiency, and exergetic efficiency.

Pevap_TFC =RefPsat_T(Fluid_TFC,Tevap_TFC)

	A	B	C	D	E	F	G	H	I	J	K	L	M	N	O
1	**Working fluids**			**TFC cycle**									**TFC**		
2	Fluid_TFC	R152a		T_hsi	93.00		s6	1.508015		h8	434.86189		Workt_TFC	656.4599	kW
3	Fluid_ORC	R152a					h7	439.22		s8	1.7098828		Workp_TFC	433.9989	kW
4	**Heating source (hot water)**			Pevap_TFC	4243.2		s7	1.7058					Worknet_TFC	222.4611	kW
5	T_hs	120	oC	Pcc_TFC	2503.08								Q_TFC	11458.8	kW
6	mflow	100	kg/s	h5	360.266		ss8	1.7058					η_TFC	1.941	%
7	ρ	943.10	kg/m3	s5	1.50023		xss8	0.40023							
8	cp	4.24	kJ/kg.K	mf_TFC	150.62947		hss8	433.4092		s_hs	1.5279		**ORC**		
9	**TFC**			v5	0.0014074	m3/kg				s_0	0.3672		Q_sensible	91.67203	kJ/kg
10	Tevap_TFC	110	oC	h6	363.1472					Exerg_hs	3472.92		Q_ORC	5413.38	kW
11	Tcc_TFC	83	oC	T6	84.214554								Workt_ORC	1416.248	kW
12	ΔTcc	3	K	**ORC cycle**									Workp_ORC	115.811	kW
13	ΔT_hs2	10	K	Tcc_ORC	80	oC	s4s	2.0198		h2	273.31119		Worknet_ORC	1300.436	kW
14	**ORC**			Pcc_ORC	2342.4	kPa	h4s	515.2144		T2	41.037827		η_ORC	7.811	%
15	Tcond_ORC	40	oC	Pcond_ORC	909.27	kPa	h4	519.4468		s2	1.2472232				
16	ΔT_sc	0.00	K				T4	40					**Overall parameters**		
17	ηt_isen	0.85		h3	543.43		s4	2.033315		h2b	261.47797		Q_total	16872.18	kW
18	ηp_isen	0.85		s3	2.0198					T2b	34.724121	kJ/kg	T_hsout	80.24	oC
19	ηx_isen	0.75		h2c	353.15		T1	40	oC	s2b	1.2098085	kg/s	Q_out	15349.28	kW
20	T_0	298.15	K	s2c	1.481		h1	271.35	kJ/kg						
21	P_0	101.325	kPa				v1	0.001163	m3/kg	Qevap_ORC	190.28	kW	W_total	1522.897	kW
22				h4b	531.28		s1	1.2411		mf_ORC	59.05	kW	η_overall	9.026	%
23				s4b	2.0711								ε_overall	43.85063	%
24															

Figure 6: The Excel-aided model for the combined cycle using R152a with the data shown on Table 1

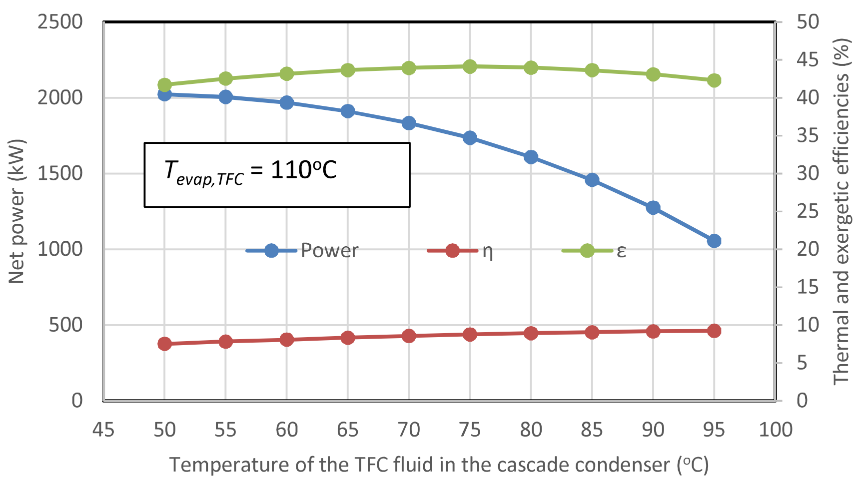

Figure 7: Variation of the combined-cycle's power and thermal and exergetic efficiencies with the temperature of the TFC fluid in the cascade condenser

5. Comparison with the simple ORC and TFC

The performance of the combined cycle will be compared to that of the ORC and TFC cycles using the same working fluid in all three cycles, which is R152a. The comparison will be for a heat-source at 120°C and using the data shown on Table 1. The comparison with the ORC will be based on its performance at the evaporator optimum temperature of 80°C as shown on Figure 4. Table 2 compares the values obtained by the three cycles for a number of performance parameters. The values relevant to the ORC and TFC have been obtained from Figure 4 and Figure 5, respectively. For the combined cycle, three sets of values are shown which correspond to three values of the temperature of the ORC fluid in the cascade condenser, Tcc_ORC, which are 70°C (CC-70), 80°C (CC-80), and 90°C (CC-90). The table figures show that the lowest exit temperature for the heat source is that of the TFC, which is 50°C, and the highest exit temperature is that of the combined cycle CC-90, which is 90.72°C.

Table 2. Performance parameters of the ORC, TFC, and the combined cycle

	TFC	ORC	CC-70	CC-80	CC-90
Ths,out (°C)	50	77.41	71.75	80.24	90.72
Qin (kW)	29708	18074.17	20479.42	16872.18	12427.7
Qout (kW)	27489.92	16600.63	18700.75	15349.28	11278.86
Power (kW)	2218.085	1473.536	1778.665	1522.897	1148.837
Thermal efficiency (%)	7.466	8.153	8.685	9.026	9.244
Exergetic efficiency (%)	38.834	25.798	31.141	43.851	20.114

Figures 8 compares amount of heat recovered, power produced, thermal efficiency, and exergetic efficiency of the three cycles. Figures 8.a and Figure 8.b show that the simple TFC recovers the most energy and produces the most power compared to the other two cycles. The figures also show that both the heat recovered and power produced by the combined cycle decrease as the cascade temperature is increased. The recovered energy and power produced by the combined cycle are lower than those of the TFC for all three cascade temperatures, but higher than that of the ORC for cascade temperatures below 80°C.

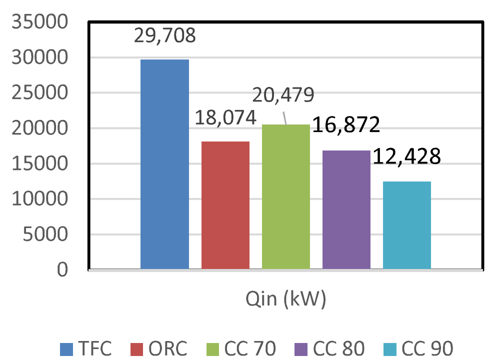

(a)

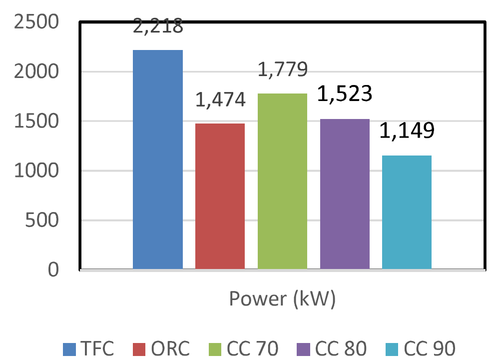

(b)

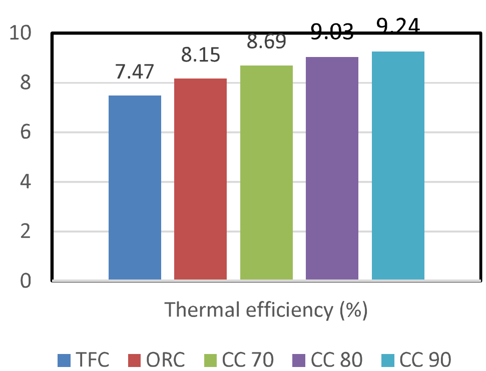

(c)

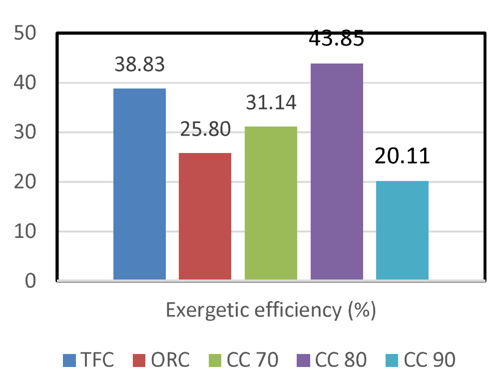

(d)

Figure 8: Comparison of (a) the recovered heating source energy, (b) the power produced, (c) the thermal efficiency, and (d) the exergetic efficiency of the combined cycle with those of the simple TFC and ORC

An unconditional advantage of the combined cycle is revealed by Figure 8.c which is that its thermal efficiency is higher than those of the TFC and ORC cycles at all three cascade temperatures and increases with the cascade temperature. Figure 8.d shows that the exergetic efficiency of the combined cycle at the cascade temperature of 80oC exceeds those for both the simple TFC and ORC cycles. These results support what has been mentioned earlier which is that there is an optimum cascade temperature for the cycle that gives the best trade-off between its power, thermal efficiency and the exergetic efficiency.

6. Conclusions

This paper presents a combined cycle for power generation from low-temperature heat sources that utilises the TFC in the high-temperature circuit and the ORC in the low-temperature circuits. By connecting the two circuits via a cascade condenser, the combined cycle allows different fluids to be used in the lower and the higher temperature ranges. The performance of the combined cycle is compared to those of the simple TFC and ORC by using an Excel-based model that utilises VBA functions to determine the refrigerants properties. The combined cycle is compared to the simple ORC and TFC by using R152a in both the HTC and LTC circuits. The results obtained for a heat source available at 120^{o}C show that combined cycle gives more power and yields higher thermal and exergetic efficiencies than the simple ORC for cascade temperatures below 80^{o}C. Compared to the simple TFC, the combined cycle produces less power, but achieves higher thermal efficiencies for any cascade temperature. The exergetic efficiency of the cycle is also higher than that of the simple TFC at a cascade temperature of 80^{o}C.

The analysis of the cycle with R152a in both the HTC and LTC shows that its thermal efficiency steadily increases by increasing the cascade temperature, but the power decreases while the exergetic efficiency has an optimum cascade temperature. Therefore, selecting the appropriate cascade temperature for the combined cycle requires a trade-off between the power of the cycle on one side and its thermal and exergetic efficiencies on the other side. Determining the most suitable cascade temperature requires multi-objecve optimisation analyses of the cycle that also take other factors into consideration including the economic, safety, and environmental factors. In this respect, the Excel-based model described in the paper allows multi-objective optimisation analyses of the cycle to be conducted by using either the free version of the MIDACO solver [17] or the Solver-TOPSIS technique described in [18].

References

[1] C. Wolf, E. Rothuizen, T. Ommen, Exergoeconomic Analysis of a Solar Powered ORC using Zeotropic Mixtures for Combined Heat & Power Generation, Proceedings of ECOS 2023 - the 36th International Conference on Efficiency, Cost,

Optimization, Simulation and Environmental Impact of Energy Systems 25-30 June, 2023, Las Palmas De Gran Canaria, Spain

[2] A.A. Bidgoli and J.I. Yanagihar, Integration of the Compression Units of the Processing Plant with an Organic Rankin Cycle for Power Generation and Cooling Process, Proceedings of ECOS 2023 - the 36th International Conference on Efficiency, Cost, Optimization, Simulation and Environmental Impact of Energy Systems 25-30 June, 2023, Las Palmas De Gran Canaria, Spain

[3] J.J. Fierro, C. Hern´andez-G´omez, C.A. Marenco-Porto, C. Nieto-Londo˜no, A. Escudero-Atehortua, M. Giraldo, H. Jouhara, L.C. Wrobel, Exergo-economic comparison of waste heat recovery cycles for a cement industry case study, Energy Conversion and Management: X 13 (2022) 100180

[4] A. Skiadopoulos, C. Antonopoulou, K. Atsonios, P. Grammelis, A. Gkountas, P. Bakalis, G. Kosmadakis, and D. Manolakos, Trilateral Flash Cycle for efficient low temperature solar heat harvesting- A case study, Proceedings of ECOS 2023 - the 36th International Conference on Efficiency, Cost, Optimization, Simulation and Environmental Impact of Energy Systems 25-30 June, 2023, Las Palmas De Gran Canaria, Spain

[5] M. Yari, A.S. Mehr, V. Zare, S.M.S. Mahmoudi, M.A. Rosen, Exergoeconomic comparison of TLC (trilateral Rankine cycle), ORC (organic Rankine cycle) and Kalina cycle using a low grade heat source, Energy 83 (2015) 712-722

[6] K-Y. Lai, Y-T. Lee, M-R. Chen and Y-H. Liu, Comparison of the Trilateral Flash Cycle and Rankine Cycle with Organic Fluid Using the Pinch Point Temperature, Entropy (2019), 21, 1197

[7] P. Lykas, C. Antonopoulou, A. Gkountas, K. Atsonios, G. Itskos, N. Nikolopoulos, P. Grammelis, D. Manolakos and P. Bakalis, Thermodynamic and economic performance of novel organic cycle designs powered by low temperature waste heat, Proceedings of ECOS 2023 - the 36th International Conference on Efficiency, Cost, Optimization, Simulation and Environmental Impact of Energy Systems 25-30 June, 2023, Las Palmas De Gran Canaria, Spain

[8] W. Sun, X. Yue, and Y. Wang. Exergy Efficiency Analysis of ORC (Organic Rankine Cycle) and ORC-Based Combined Cycles Driven by Low-Temperature Waste Heat. Energy Conversion and Management, 135, (2017), 63-73. https://doi.org/10.1016/j.enconman.2016.12.042

[0] N. Toujani, N. Bouaziz, M. Chrigui, L. Kairouani, Performance analysis of a new combined organic Rankine cycle and vapor compression cycle for power and refrigeration cogeneration, Transactions of the Institute of Fluid-flow Machinery, No. 140, 2018, 39–81

[10] C.O.C. Oko, M.M. Deebom, and, E.O. Diemuodeke, Exergoeconomic analysis of cascaded organic power plant for the Port Harcourt climatic zone, Nigeria, Cogent Engineering (2016), 3: 1227127, http://dx.doi.org/10.1080/23311916.2016.1227127

[11] G. Liu, Q. Wang, J. Xu, Z. Miao. Exergy Analysis of Two-Stage Organic Rankine Cycle Power Generation System. Entropy 2021, 23, 43. https://doi.org/10.3390/e23010043

[12] Y.S.H. Najjar, A.E. Qatramez. Energy utilisation in a combined geothermal and organic Rankine power cycles. Int. J. Sustain. Energy 2019, 38, 831–848.

[13] N. Hassani Mokarram, A.H. Mosaffa. Investigation of the thermoeconomic improvement of integrating enhanced geothermal single flash with transcritical organic Rankine cycle. Energy Convers. Manag. 2020, 213, 112831.

[14] J.C. Jiménez-García, A. Ruiz, A. Pacheco-Reyes, W.A. Rivera, Comprehensive Review of Organic Rankine Cycles. Processes 2023, 11, 1982. https://doi.org/10.3390/pr11071982

[15] S. Trædal, Analysis of the Trilateral Flash Cycle for Power Production from Low Temperature Heat Sources. Master's Thesis, Institutt for Energi-og Prosessteknikk, Kolbjørn Hejes v 1B, Trondheim, 2014.

[16] C.O.C. Oko and, E.O. Diemuodeke, MS Excel spreadsheet add-in for thermodynamic properties and process simulation of R152a, Energy Science and Technology, Vol. 5, No. 2, 2013, pp. 63-69.

[17] MIDACO-Solver, http://www.midaco-solver.com/

[18] M.M. El-Awad, A Solver-TOPSIS technique for multi-objective optimisation of innovative multi-stage VCR systems by using Microsoft Excel, Journal of Engineering Research. Faculty of Engineering-University of Tripoli, Issue (38), November 2024, 25-42, https://www.jer.ly/search_articles.php?f=38

[19] M.J, Moran and H.N. Shapiro, Fundamentals of Engineering Thermodynamics, 5th edition, John Wiley, & Sons. Inc. 2006

[20] M.M. El-Awad, A Multi-Subject Excel Add-In for Fluid Properties and its Use for analysing Cascade and Multi-Stage Compression Refrigeration Cycles, The Electronic Journal of Spreadsheets in Education (eJSiE) Vol. 12, Issue 1, April 18, 2019

[21] ASHRAE Handbook–Refrigeration, 2017, American Society of Heating, Refrigerating and Air-Conditioning Engineers, Inc., (SI Edition).

[22] M.M. El-Awad, M.S. Al Nabhani, K.S. Al Hinai, A. Younis. 2019. Development and Validation of an Excel Add-In for Determining the Properties of Various Refrigerants, Proceedings of First National Conference on Recent Trends in Applied Science, Engineering and Technology (CASET 2K19), Ipri College of Technology, June 11, 2019.

[23] H. Atalay, M.T. Coban, Modeling of Thermodynamic Properties for Pure Refrigerants and Refrigerant Mixtures by Using the Helmholtz Equation of State and Cubic Spline Curve Fitting Method , Universal Journal of Mechanical Engineering 3(6), 2015: 229-251, http://www.hrpub.org

[24] A. D. Parekh and P. R. Tailor, Thermodynamic Analysis of R507A-R23 Cascade Refrigeration System, World Academy of Science, Engineering and Technology

International Journal of Mechanical and Mechatronics Engineering Vol:5, No:9, 2011